

Sub-Arcsecond Near-Infrared Images of Massive Star Formation Region NGC 6334 V*

Jun HASHIMOTO,^{1,2} Motohide TAMURA,^{1,4} Hiroshi SUTO,¹ Lyu ABE,¹
Miki ISHII,³ Tomoyuki KUDO,⁴ Satoshi MAYAMA⁴

¹National Astronomical Observatory, 2-21-1 Osawa, Mitaka, Tokyo 181-8588; hashmtjn@optik.mtk.nao.ac.jp

²Department of Physics, Tokyo University of Science, 1-3, Kagurazaka, Shinjuku-ku, Tokyo 162-8601

³Subaru Telescope, 650 North A'ohoku Place, Hilo, HI 96720

⁴Department of Astronomical Science, Graduate University for Advanced Studies (Sokendai),
2-21-1 Osawa, Mitaka, Tokyo 181-8588

(Received ; accepted)

Abstract

We present high spatial resolution ($0''.3$) polarimetric images in the H and K bands and direct images in the L' and M' bands of the NGC 6334 V infrared nebulae. The images show complex structures including the multi-shells and various knots in the nebulae. The appearances and colors of the eastern and western nebulae differ considerably. Our polarization images also show differences between the illuminating sources of the nebulae: the eastern nebula is illuminated by a deeply embedded mid-infrared source, KDJ 4, and the western nebula by our newly detected near-infrared source, WN-A1. The degree of polarization of the nebulae is very large, up to 70% at K and 60% at H , which is consistent with a single scattering of near-infrared radiation from each source at the walls of the mass outflows.

Key words: stars: formation — polarization — ISM: individual (NGC 6334 V)

1. Introduction

NGC 6334 V is one of the far-infrared sources (total luminosity of $L \sim 10^5 L_\odot$; Loughran et al. 1986) along the ridge of the massive star-formation regions in the NGC 6334 complex at a distance of 1.7 kpc (Neckel 1978). Fischer et al. (1982) detected 2 μm and 2.6 mm emission from H_2 and CO, respectively. Near the H_2 emission region, Harvey and Wilking (1984) found an IR bipolar nebula. Simon et al. (1985) and Kraemer et al. (1999) showed that four IR sources (IRS V-1 detected at 3.5 μm and 12.5 μm , V-2 at 3.5 μm , 12.5 μm and 20.6 μm , V-3 at 3.5 μm , 12.5 μm and 20.6 μm , KDJ 4 at 12.5 μm and 20.6 μm) along the ridge of the nebula, which made it difficult to identify the nebula's source of illumination.

Several polarimetric observations of NGC 6334 V have been carried out. Polarization studies can indicate the sources of illumination of the reflection nebula in star formation regions. However, because of crowding of several sources, previous polarimetric observations of this region were unable to identify the source(s) convincingly:

1. Simon et al. (1985) measured IR aperture polarizations in the H and K bands of IRS V-1. They measured a degree of polarization at H of $P_H \sim 59\%$ at position angle $\theta_H \sim 160^\circ$, and P_K of $\sim 46\%$ at $\theta_K \sim 165^\circ$. They suggested that the large polarization of IRS V-1 was due to illumination by IRS V-2 or V-3.

2. Wolstencroft, Scarrott & Warren-Smith (1987) measured optical polarizations of OS1 which coincided with

IRS V-2. They found $P_{\text{opt}} \sim 38\%$ at $\theta_{\text{opt}} \sim 160^\circ$. They concluded that the illuminating source of OS1 was IRS V-3 and that IRS V-3 was likely the illuminating source of the IR bipolar nebula.

3. Nakagawa et al. (1990) measured L' band polarizations of the bipolar nebula. They found a symmetric polarization vector pattern of the bipolar nebula illuminated by a central star. They concluded that the source of the nebula was the 20 μm peak which was identified with IRS V-3 in Simon et al. (1985).

4. Chrysostomou et al. (1994) measured H , K_n and nbL bands polarizations of the bipolar nebula. At the peaks of the eastern nebula, they found P to be $\sim 60\%$ in the H and K_n bands with $\theta \sim 160^\circ$. In the western nebula they found a centrosymmetric polarization vector pattern polarized $\sim 50\%$ in the K_n band, while P was $\sim 20\%$ in the H band. They concluded that the centrosymmetric polarization vector pattern in the western nebula was due to illumination by IRS V-3. Since the polarization vector pattern of the eastern nebula was not centrosymmetric, they could not identify the illuminating source of the eastern nebula.

In general, the observations of distant star-formation regions require high spatial resolutions. All the above polarimetric observations were conducted at over $1''$ spatial resolutions. Considering both the large distance to NGC 6334 V and the crowding of the cluster of IR sources, high-resolution imaging is essential to study of this IR nebula. Thus we performed high resolution polarimetry in the H and K bands and imaging in the H , K , L' and M' bands.

* Based on data collected at the Subaru Telescope, which is operated by the National Astronomical Observatory of Japan.

Table 1. Near-IR, mid-IR and radio sources in NGC 6334 V

IR knot This paper	Simon et al. (1985)	Kraemer et al. (1999)	Rengarajan & Ho (1996)	RIGHT ASCENSION* (J2000)	DECLINATION* (J2000)
EN-A1	IRS V-1	KDJ 1	R E-2	17 19 58.201	-35 57 49.37
EN-A2	IRS V-2	KDJ 2	...	17 19 58.066	-35 57 50.30
EN-A3	17 19 58.305	-35 57 49.53
WN-A1	...	(KDJ 3)	...	17 19 57.785	-35 57 50.81
WN-A2	...	(KDJ 3)	...	17 19 57.790	-35 57 49.84
...	...	KDJ 4	R E-3 ‡	17 19 57.461 † ‡	-35 57 52.47 † ‡

* Positional errors are estimated to be less than $0''.1$.

† Absolute position is for KDJ 4.

‡ Absolute position for R E-3, $17^{\text{h}}19^{\text{m}}57^{\text{s}}.55, -35^{\circ}57'51''.57$ (J2000), is estimated by assuming that R E-2 coincides with EN-A1 (see §3.2 in the text).

2. Observations and Data reduction

H and K polarimetry and L' and M' imaging of the NGC 6334 V IR nebula were conducted on the Subaru telescope with CIAO (Tamura et al. 2000; Murakawa et al. 2004) on 2005 June 27. The pixel scale of CIAO was 0.0213 arcsec pixel $^{-1}$. The details of the polarimeter have been described elsewhere (Tamura et al. 2003). Although no adaptive optics were employed in these observations, the good and stable seeing enabled us to achieve a high spatial resolution $0''.3$ in the H , K , L' and M' bands. The polarizations were measured by stepping the half waveplate at four angular positions (0° , 45° , 22.5° and 67.5°). We took 3 frames of $20 \text{ s} \times 6$ co-adds integration per waveplate position in the H and K bands, 4 frames of $0.5 \text{ s} \times 100$ co-adds integration in the L' band, and 8 frames of $0.2 \text{ s} \times 100$ co-adds integration in the M' band.

The data were reduced in the standard manner of infrared image reduction: subtracting a dark-frame and dividing by a flat-frame. In addition, the data for each waveplate position (I_0 , I_{45} , $I_{22.5}$ and $I_{67.5}$) were registered, and then combined. Stokes I , Q , U parameters, degree of polarization (P), and position angle (θ) are calculated as follows (see e.g., Tamura et al. 2003).

$$I = \{I_0 + I_{45} + I_{22.5} + I_{67.5}\} / 2,$$

$$Q = I_0 - I_{45}, \quad U = I_{22.5} - I_{67.5},$$

$$P = \sqrt{\left(\frac{Q}{I}\right)^2 + \left(\frac{U}{I}\right)^2}, \quad \text{and } \theta = \frac{1}{2} \arctan\left(\frac{U}{Q}\right).$$

3. Results and Discussion

3.1. Imaging observations

Figures 1(A) and (B) show the central region of NGC 6334 V obtained with Subaru/CIAO. In addition, Figure 1(C) shows a large scale structure of this region taken with SIRIUS (Nagayama et al. 2003), a simultaneous three color infrared camera, on the IRSF 1.4m telescope in Sutherland, South Africa. There are four distinct nebulae associated with NGC 6334 V. We refer to them as in figure 1(C), e.g., Eastern Nebula A, or EN-A.

In Figures 1(A) and (B), the structure of the bipolar nebula is complicated. The shape of EN-A is a

paraboloidal cone centered at $(-4'', -1'')$ with several bright knots, while WN-A has a multi-shell structure with a bright western edge. It is the first time that these fine structures in NGC 6334 V have been detected. Few previous observations have detected a multi-shell structures (e.g., GL 2591, Tamura & Yamashita 1992).

A schematic view of the structures is shown in Figure 1(D). Moreover, the colors of EN-A and WN-A differ systematically. Figure 1(E) shows that EN-A is bluer ($H - K \sim 3$ mag) than WN-A ($H - K \sim 4$ mag); EN-A was detected in the J , H , K , L' and M' bands, while WN-A was detected in the K , L' and M' bands. Due to a high extinction, WN-A was detected only faintly with CIAO in the H band.

In Figures 1(A) and (B), there are several bright knots which we refer to as in Figure 1(D), e.g., EN-A1. Table 1 summarizes names of these near-IR knots and their absolute positions. Each position was measured as follows: we measured the relative position of the knots based on the IRSF/SIRIUS data, and we used the absolute position of a reference star from 2MASS-PSC. The position of the reference star is marked in Figure 1 (C).

3.2. Identifications with previous sources

Simon et al. (1985) reported three near- and mid-IR ($3.5 \mu\text{m}$ and $20 \mu\text{m}$) sources, IRS V-1, V-2 and V-3. The positions for IRS V-1 and V-2 do not exactly coincide with our new positions for EN-A1 and A2, respectively, though they are close with each other. Their relative positions agree well with each other. Thus if we assume that EN-A1 coincides with IRS V-1, EN-A2 comes to coincide with IRS V-2. That is why we identify EN-A1 and A2 with IRS V-1 and V-2, respectively. However, we can see no counterpart to IRS V-3. Since IRS V-3 lies at a middle position between the newly detected WN-A1 and A2, we suggest that our high spatial resolution observations allow IRS V-3 to be resolved into WN-A1 and A2. L' and M' magnitudes of WN-A1 are 10.54 ± 0.02 and 9.43 ± 0.04 mag, respectively, while K , L' and M' magnitudes of WN-A2 are 12.68 ± 0.02 , 9.94 ± 0.02 and 9.29 ± 0.03 mag, respectively. The positions of IRS V-1 to V-3 are plotted in Figure 1 (D), as well.

Kraemer et al. (1999) reported four mid-IR ($12.5 \mu\text{m}$ and $20.6 \mu\text{m}$) sources, KDJ 1 to 4. As with the above

discussion, since relative positions of KDJ 1 and 2 with respect to EN-A1 and A2 agree well with each other, we identify EN-A1 and A2 with KDJ 1 and 2, respectively. In addition, KDJ 3 also corresponds to WN-A1 and A2 collectively. Since we have no near-IR counterpart to KDJ 4, the relative position of KDJ 4 with respect to KDJ 1 was converted to an absolute position in Table 1.

Rengarajan & Ho (1996) reported three radio continuum (2 cm) sources. Since R E-2 coincided with IRS V-1, we identified R E-2 with EN-A1. As with the position of KDJ 4, the relative positions of R E-3 with respect to R E-2 was converted to absolute positions. Note that R E-3 was identified with KDJ 4 (Kraemer et al. 1999). R E-1 has no new near- and mid-IR counterpart and its nature is unknown. Thus, we do not discuss on this source.

3.3. Imaging polarimetric observations

Figure 2 shows the various polarization images in the H and K bands, and table 2 summarizes the measured degrees of polarization. We observed a very large degree of polarization for the nebulae in the H and K bands. At the peak of EN-A we obtained $\sim 65\%$ in the H band and $\sim 70\%$ in the K band. WN-A is polarized at $\sim 60\%$ in the K band. These results are consistent with those of Chrysostomou et al. (1994), but we obtained a slightly higher degree of polarization than their values. We consider that this is due to our high resolution ($0''.3$).

Table 2. Degrees of polarization in the H and K bands

nebula	this paper	Chrysostomou et al. (1994)
EN-A (H band)	$\lesssim 65\%$	$\lesssim 60\%$
EN-A (K band)	$\lesssim 70\%$	$\lesssim 60\%$
WN-A (H band)	—	$\lesssim 20\%$
WN-A (K band)	$\lesssim 60\%$	$\lesssim 50\%$

Figure 2(C) shows that polarization vector pattern in EN-A and WN-A differ considerably. In WN-A, the polarization vector patterns are centrosymmetric, while in EN-A, the vectors are relatively well aligned with each other, $\theta \sim 160^\circ$. In order to determine the sources of illumination of EN-A and WN-A, the polarization vectors were rotated 90° , and extended as shown in Figures 3(A) and (B). Figures 3(A) and (B) show the average position of all intersections with 1σ error box. The errors of the polarization vector patterns arisen from the sky noise are quite small. The above procedure was based on the seeing size rather than on each pixel. In order to identify which source illuminates the nebulae, the error boxes in Figure 3(A) and (B) are superposed on as shown in Figure 3(C), (D) and (E); NIR composite image (C), MIR contour (D) and $\text{NH}_3(3,3)$ emission contour (E).

Since both WN-A1 and KDJ 4 lie close to the error boxes, we conclude that the WN-A is illuminated by WN-A1, and EN-A is by KDJ 4. Kraemer et al. (1999) suggested that KDJ 3 and 4 coincided with the two $\text{NH}_3(3,3)$

clumps within the positional accuracy. No additional IR-invisible sources seem to be necessary to interpret our polarization data.

Figures 2(B) and 2(D) show that EN-A1 to EN-A3 and WN-A2 have more than 50 % polarization, which implies that these knots are not self-luminous in the H and K bands. We suggest that these knots seem to be near-infrared single-scattering radiation from each relatively high-density region at the walls of the outflows (Nakagawa et al. 1990). Nakagawa et al. (1990) explained the exceptionally large (up to $\sim 100\%$) degree of polarization in the L' band by considering a simple lobe model; the scattering occurred only at the surface of the lobe. It has been suggested that there is a close relationship between infrared reflection nebosity (IRN) and CO bipolar outflow (Yamashita et al. 1989). Polarimetry toward the central infrared source of CO bipolar outflows shows a polarization perpendicular to the outflow direction (Sato et al. 1985). Viewed at low spatial resolution, the extension of IRN tends to be consistent with that of CO outflow (Tamura et al. 1990). In this NGC 6334 V region, Fischer et al. (1982) have shown a CO outflow and Straw, Hyland & McGregor (1989) found evidence that this outflow has triggered further star-formation activity via interaction with the ambient cloud material. Thus we suggest that EN-A and WN-A are IRNe which are the walls of molecular outflows. A position-velocity CO map centered on IRS V-3 of Fischer et al. (1982) showed that two peaks of blueshifted emission were located in the vicinity and both sides of IRS V-3, which consistent with our results. Our polarimetric results imply that there are two independent outflows in NGC 6334 V region.

3.4. Natures of the two "outflow" sources and other near-IR sources.

Among the six IR sources, the outflow source KDJ 4 which coincides with 2 cm continuum source R E-3 is identified to be a B2 zero-age main-sequence (ZAMS) star (Rengarajan & Ho 1996; Kraemer et al. 1999). Another outflow source WN-A1, however, is not associated with a radio continuum source (Rengarajan & Ho 1996), but with (part of) an mid-IR source KDJ 3 and the ammonia clump. Therefore, we suspect this to be a massive embedded YSO with a dense core.

EN-A1 is also associated with a radio continuum source (R E-2), thus suggested to be a B-type ZAMS star (Jackson & Kraemer 1999). However, in §3.3, we mentioned that EN-A1 was a reflection nebula. Since there is no clear change of near-IR polarization pattern over the "self-luminous" star EN-A1, we suggest that the scattered light from KDJ 4 is more dominant than the brightness of EN-A1 at near-IR. By contrast, EN-A2 and WN-A2 (KDJ 2 and part of KDJ 3, respectively) are not associated with radio continuum sources (Rengarajan & Ho 1996) and not temperature peaks (Kraemer et al. 1999), therefore are knots of the near-IR reflection nebula. Similarly, EN-A3 seems to be a simply peak of the near-IR reflection nebula.

Therefore, our observations, combined with previous mid-IR and radio observations, have revealed the presence

of at least three clustered YSOs in the NGC 6334 V, of which two YSOs are probably powering massive outflows. Further high spatial resolution CO observations should be undertaken to reveal the kinematics of these outflows.

4. Conclusion

We conducted Subaru/CIAO direct and polarimetric imaging of the NGC 6334 V nebulae; Eastern Nebula A (EN-A) and Western Nebula A (WN-A), with a high resolution of $0''.3$. We detected two red near-IR sources (WN-A1 and A2) near the position of mid-IR source KDJ 3. We found that EN-A and WN-A are illuminated by the different infrared sources of KDJ 4 and WN-A1, respectively. Combined with previous mid-IR and radio observations, we suggest that the outflow sources of KDJ 4 and WN-A1 are a B-type ZAMS star and a massive embedded YSO with a dense core, respectively. In addition, fine structures of both nebulae were detected; in particular, we found that the western nebula has a multi-shell structure. The high levels of polarization of EN-A2 and WN-A2 in the K band suggest that these are not self-luminous, but rather knots of the reflection nebulae.

We are grateful to Misato Fukagawa for several useful comments on an earlier version of this paper. We also thank an anonymous referee for providing many useful comments that lead to a significantly improved paper. This research was partly supported by MEXT Japan, Grant-in-Aid for Scientific Research on Priority Areas, "Development of Extra-solar Planetary Science".

References

- Chrysostomou, A., Hough, J. H., Aspin, C., & Bailey, J. A. 1994, MNRAS, 268, L63.
- Fischer, J., Joyce, R. R., Simon, M., & Simon, T. 1982, ApJ, 258, 165.
- Harvey, P. M. & Wilking, B. A. 1984, ApJL, 280, L19.
- Jackson, J. M. & Kraemer, K. E. 1999, ApJ, 512, 260.
- Kraemer, K. E., Deutsch, L. K., Jackson, J. M., Hoffmann, W., Hora, J., Dayal, A., & Fazio, G. 1999, ApJ, 516, 817.
- Loughran, L., McBreen, B., Fazio, G. G., Rangarajan, T. N., Maxson, C. W., Serio, S., Sciortino, S., & Ray, T. P. 1986, ApJ, 303, 629.
- Neckel, T. 1978, A&A, 69, 51.
- Murakawa, K., et al. 2004, PASJ, 56, 509.
- Nagayama, T., et al. 2003, Proc. SPIE, 4841, 459.
- Nakagawa, T., Nagata, T., Matsuhara, H., Okuda, H., Shibai, H., & Hayashi, S. S. 1990, ApJ, 351, 573.
- Rangarajan, T. N. & Ho, P. T. P. 1996, ApJ, 465, 363.
- Simon, T., Dyck, H. M., Wolstencroft, R. D., Joyce, R. R., Johnson, P. E., & McLean, I. S. 1985, MNRAS, 212, 21p.
- Straw, S. M., Hyland, A. R., & McGregor, P. J. 1989, ApJS, 69, 99.
- Sato, S., Nagata, T., Nishida, M., Tanaka, M., & Yamashita, T. 1985, ApJ, 291, 708.
- Tamura, M., Sato, S., Suzuki, H., Kaifu, N., & Hough, J. H. 1990, ApJ, 350, 728.
- Tamura, M. & Yamashita, T. 1992, ApJ, 391, 710.
- Tamura, M., et al. 2000, Proc. SPIE, 4008, 1153.
- Tamura, M., Fukagawa, M., Murakawa, K., Suto, H., Itoh, Y., & Doi, Y. 2003, Proc. SPIE, 4843, 190.
- Wolstencroft, R. D., Scarrott, S. M., & Warren-Smith, R. F. 1987, MNRAS, 228, 805.
- Yamashita, T., Suzuki, H., Kaifu, N., Tamura, M., Mountain, C. M., & Moore, T. J. T. 1989, ApJ, 347, 894.

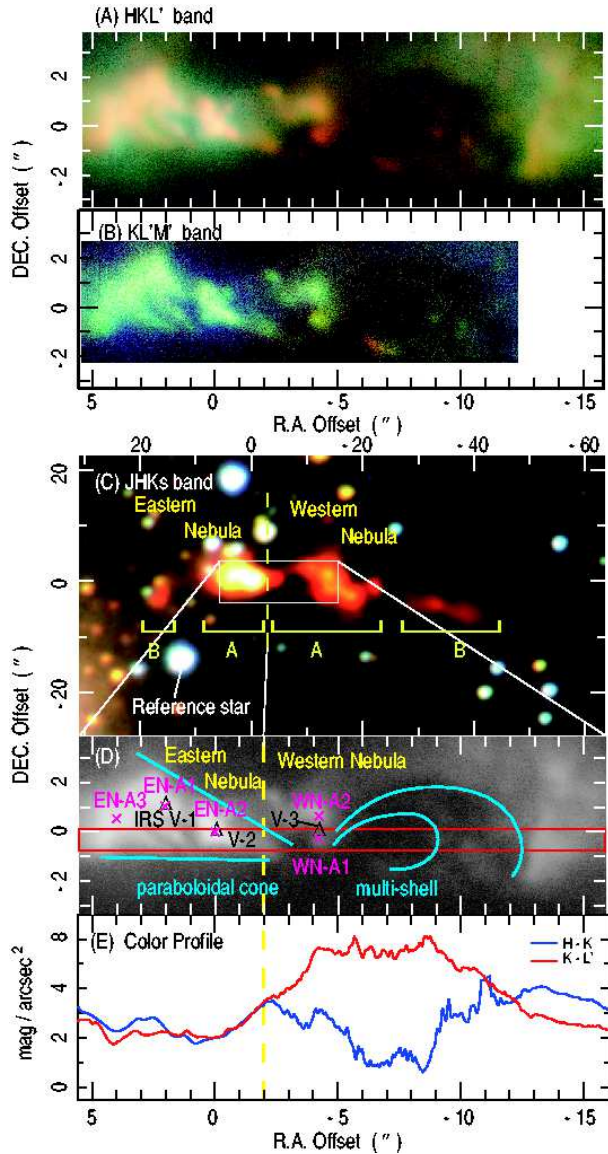


Fig. 1. (A) : The three-color composite image of the intensity in the H , K and L' bands (H :blue, K :green, L' :red) obtained with Subaru/CIAO. Only a center region of $21'' \times 7''$ of the CIAO field is shown here. (B) : The same as (A) but in the K , L' and M' bands (K :blue, L' :green, M' :red). (C) : The same but in the J , H and K_s band (J :blue, H :green, K_s :red) obtained with IRSF/SIRIUS. Only a region of $\sim 100'' \times 50''$ of the SIRIUS field is shown here. (D) : The same as (A) but this frame shows the sketch of the EN-A1 and WN-A1; a paraboloidal cone and a multi-shell structure are outlined (blue line). Also shown are the positions of the peak of the bright knots (pink crosses) and IRS V-1 to V-3 in the $3.5 \mu\text{m}$ and $20 \mu\text{m}$ (black triangles; Simon et al. 1985). Red rectangle represents a locus of the cut for a color-profile in (E). (E) : A color profile of $H - K$ and $K - L'$ magnitudes averaged over the red box in (D). In these all figures, the positional offsets are relative to the peak at EN-A2 in the H and K ; $(0'', 0'') = 17^{\text{h}} 19^{\text{m}} 58^{\text{s}}.1, -35^{\circ} 57' 50''$ (J2000).

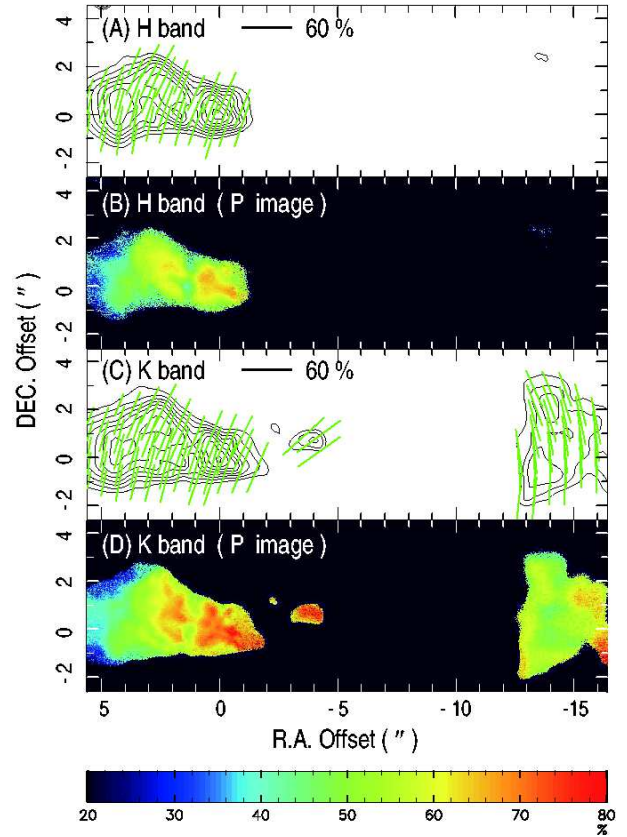


Fig. 2. (A) : H band polarization image overlaid with contours of intensity. (B) : The degrees of polarization P in the H band. (C) : The same as (A) but in the K band. (D) : The same as (B) but in the K band. In these all figures, the $(0'', 0'')$ coordinates are the same as in Figure 1.

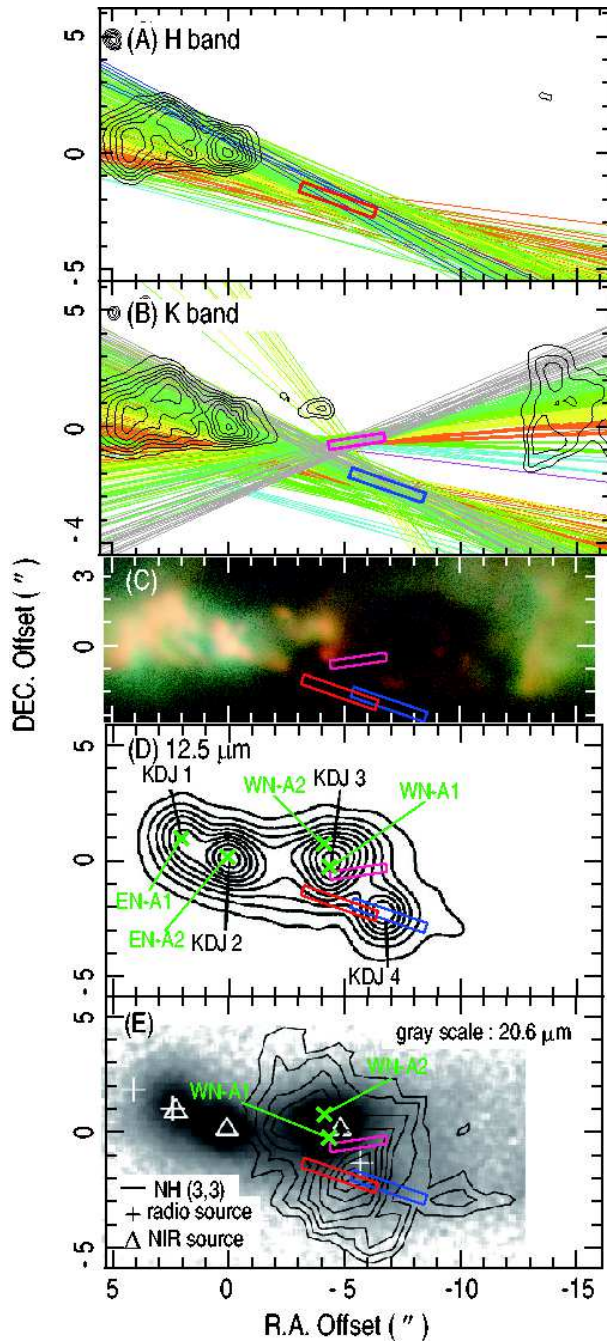


Fig. 3. (A): *H* band polarization image overlaid with contours of total intensity. The vectors have been rotated 90° and extended to indicate the source of the illumination of EN-A. The 1σ error box shows this location. The color of the vectors are changed for presentation purpose. (B): The same as (A) but in the *K* band. (C): The positions of the illuminating sources superposed on the *H*, *K* and *L'* composite-image obtained with CIAO. (D): Those superposed on the $12.5\ \mu\text{m}$ contour of Kraemer et al (1999). In addition, The positions of WN-A1, WN-A2, EN-A1 and EN-A2 are marked (green crosses of \times). (E): Those superposed on the $\text{NH}_3(3,3)$ line intensity and the $20\ \mu\text{m}$ emission of Kraemer et al. (1999). The positions of additional features are marked; WN-A1 and A2 (green crosses of \times), IRS V-1 to V-3 (left to right) at $3.5\ \mu\text{m}$ and $20\ \mu\text{m}$ (white triangles of Δ ; Simon et al. 1985), R E-1 to E-3 (left to right) of $2\ \text{cm}$ continuum (white crosses of $+$; Rengarajan & Ho 1996). In these all figures, the $(0'', 0'')$ coordinates are the same as in Figure 1. Note that the position of IRS V-3 is displaced from that in the original figure of Kraemer et al. (1999) (see §3.2 in the text).